Crystal Structure and Subunit Dynamics of the Abalone Sperm Lysin Dimer: Egg Envelopes Dissociate Dimers, the Monomer Is the Active Species

A. Shaw,* P. A. G. Fortes,‡ C. D. Stout,* and V. D. Vacquier§

*Department of Molecular Biology, The Scripps Research Institute, La Jolla, California 92037-1093, ‡Department of Biology and §Marine Biology Research Division, University of California, San Diego, La Jolla, California 92093

Abstract. Lysin is a 16-kD acrosomal protein used by abalone spermatozoa to create a hole in the egg vitelline envelope (VE) by a nonenzymatic mechanism. The crystal structure of the lysin monomer is known at 1.9Å resolution. The surface of the molecule reveals two tracks of basic residues running the length of one surface of the molecule and a patch of solvent-exposed hydrophobic residues on the opposite surface. Here we report that lysin dimerizes via interaction of the hydrophobic patches of monomers. Triton X-100 dissociates the dimer. The crystal structure of the dimer is described at 2.75 Å resolution. Fluorescence energy transfer experiments show that the dimer has an approximate K_D of 1 μM and that monomers exchange rapidly between dimers. Addition of isolated egg VE dissociates dimers, implicating monomers as the active species in the dissolution reaction. This work represents the first step in the elucidation of the mechanism by which lysin enables abalone spermatozoa to create a hole in the egg envelope during fertilization.

During fertilization, spermatozoa must penetrate the extracellular investments surrounding the egg before the plasma membranes of the two gametes can make contact and fuse. To accomplish this, most animal species have evolved sperm with acrosomal vesicles that undergo exocytosis to release lytic proteins used in penetration of the egg coat. Abalone spermatozoa possess an enormous acrosomal vesicle (Lewis et al., 1980). These sperm bind to the elevated egg vitelline envelope (VE)[1] and release concentrated 16-kD lysin from the exocytosing acrosome. Lysin creates a hole in the VE by a nonenzymatic mechanism to allow the sperm cell to pass through the VE and fuse with the egg (Lewis et al., 1982).

Purified lysin exhibits species-selectivity in the dissolution of isolated VE. For example, 12 μg of red abalone (*Haliotis rufescens*) lysin will dissolve 95% of red abalone egg VE, whereas 12 μg of lysin from the black abalone (*H. cracherodii*) is ineffective against red abalone VE. Red abalone lysin is also ineffective at dissolving pink abalone (*H. corrugata*) VE (Vacquier and Lee, 1993). The seven species of Eastern Pacific (California Coast) abalone have overlapping habitats and breeding seasons. The species-selectivity of lysin in dissolving the egg VE may be one mechanism that has evolved to establish prezygotic reproductive isolation among abalone species (Vacquier and Lee, 1993; Lee, 1994; Lee et al., 1995). To cell biology, the species-selective interaction between abalone sperm lysin and the egg VE represents a unique experimental model for studying molecular recognition between two cells.

The deduced amino acid sequences of lysin (mature lysins are 126–138 residues) from 20 species of abalones from various global locales show that the NH_2-terminal domain of residues 1–12 is always species unique, suggesting that it is the domain of lysin most important in species-selective recognition of the VE (Lee et al., 1995). Monomeric lysin is the first fertilization protein whose crystallographic structure has been solved (Shaw et al., 1993). Resolved at 1.9 Å, several striking features are seen. The monomer is composed of a tight bundle of α-helices forming a novel fold with no β sheet and no binding pocket or cleft. The species-unique domain of residues 1–12 extends away from the helical bundle. Two parallel tracks of basic residues (1 of 9 and the other 14 residues) run the length of one surface of the protein and the opposite surface possesses a patch of 11 solvent-exposed hydrophobic residues (Shaw et al., 1993). The presence of the basic tracks and the hydrophobic patch suggested the hypothesis that lysin

Dr. Shaw's present address is Genencor International, South San Francisco, California 94080.

Address all correspondence to Dr. Victor D. Vacquier, Marine Biology Research Division 0202, University of California, San Diego, La Jolla, California 92093. Tel.: (619) 534-4803. Fax: (619) 534-7313. e-mail: vvacquier@ucsd.edu.

1. *Abbreviations used in this paper*: DSP, dithiobis(succinimidylpropionate); FITC, Fluorescein-5-isothiocyanate; 1F+4R, one part FITC-lysin plus four parts RITC-lysin, both at equal molar concentrations in seawater; Mes, morpholino-ethane sulfonic acid; VE, isolated vitelline envelopes from abalone eggs.

may act by competitively disrupting both hydrogen bonds and hydrophobic interactions among VE glycoproteins.

Here we report that at physiological concentrations, lysin exists as a homodimer by interaction of apposing hydrophobic patches of monomers. The crystal structure of the dimer resolved at 2.75 Å is described. Fluorescence energy transfer experiments show that the K_D for dimer formation is ~1 μM and that monomers exchange rapidly between dimers. Addition of isolated egg VE results in the dissociation of dimers. The data are consistent with the hypothesis that the monomer is the active species in the dissolution of egg envelopes during fertilization.

Materials and Methods

Isolation of Lysin, Radioiodination and Chemical Cross-linking

Lysin was isolated from spermatozoa of the red abalone, *Haliotis rufescens*, by mincing dissected testes in seawater (all seawater was passed through a 0.45-μm filter), filtering the cell suspension through cheesecloth and sedimenting the sperm at 1,000 *g* for 20 min (4°C). The cells were suspended in 25 vol of seawater containing 0.5% vol/vol Triton X-100 that extracts the acrosomal proteins (30 min). After centrifugation at 30,000 *g* for 30 min the supernatant was dialyzed against a minimum of 100 vol of 250 mM NaCl/10 mM morpholino-ethane sulfonic acid (Mes), pH 6.0 (NaCl/Mes). After dialysis, the sample was centrifuged as above and the supernatant loaded onto a 60 ml bed (2.5-cm-diam) of CM-cellulose equilibrated in NaCl/Mes. The column was washed with at least 10 vol NaCl/Mes containing 1% vol/vol Triton X-100/1% vol/vol mercaptoethanol, followed by 10 vol of NaCl/Mes containing 3 M urea, and finally a minimum of 20 vol of NaCl/Mes alone. The column was eluted by a linear gradient of 200 ml 250 mM NaCl/10 mM Mes/pH 6.0 vs. 200 ml of 1250 mM NaCl/10 mM Mes/pH 6.0 and 5-ml fractions taken every 2.5 min. The purified lysin peak eluted at ~600 mM NaCl and gave a heavy Coomassie Blue staining band when analyzed by SDS-PAGE (Vacquier and Lee, 1993). The peak fractions were used for crystal growth without further purification.

To radioiodinate lysin, two ml of a seawater solution of lysin at 1 mg/ml were placed in a round bottom 50-ml plastic tube and 2 mCi of carrier-free $Na^{125}I$ (Amersham Corp., Arlington Heights, IL) added. Two Iodobeads® (Pierce Chemical Co., Rockford, IL) were added and the tube rocked for 10 min at 23°C. The labeled lysin was dialyzed extensively against seawater/0.04% sodium azide to remove free iodide. The labeled protein retained its ability to dissolve isolated egg VE. The specific activity was diluted so that 5 μl contained 1 μg of lysin that had ~250,000 cpm.

Chemical cross-linking was used to show that lysin is a dimer in solution and that Triton X-100 and other detergents dissociate the dimer. 25-μl portions of seawater were placed in a series of 1.5-ml microfuge tubes. 25 μl of a 1% vol/vol solution of Triton X-100 in seawater was titered down in these tubes with a 50% dilution per transfer. 5 μl (1 μg) of ^{125}I-lysin were added to each tube, bringing the volume to 30 μl. The final concentration of lysin was 2.05 μM (all molarities of lysin in this report are based on the monomeric molecular weight of 16,083, obtained by mass spectroscopy) and the concentration of Triton X-100 ranged from 0.0005% to 0.83% vol/vol. After a minimum of 30 min incubation at 23°C, 2 mg of the cross-linker dithiobis(succinimidylpropionate) (DSP; Pierce Chemical Co.) was dissolved in 500 μl dimethysulfoxide (10 mM). This DSP stock was immediately added to 15.5 ml of seawater and 30-μl portions added to the radiolabeled lysin in the Triton X-100 concentration series, making the final concentration of DSP 156 μM. After 10 min the cross-linker was inactivated by addition of 60 μl of Laemmli (1970) sample buffer without mercaptoethanol. 50-μl portions of each tube were electrophoresed on a 10% polyacrylamide gel (Laemmli, 1970), stained with Coomassie Blue, destained, dried, and an autoradiogram of the gel obtained. In some gels the radioactivity in dimer and monomer bands was determined by excising the bands from dried gels and gamma counting. The activity of lysin to dissolve isolated egg VE was quantitatively determined in the light scattering assay (Lewis et al., 1982; Vacquier and Lee, 1993).

Crystallographic Methods

Crystals of lysin grown at pH 5.5 contain two molecules per asymmetric unit and belong to the orthorhombic space group $P222_1$ with cell constants a = 51.2 Å, b = 47.0 Å, and c = 123.8 Å (52% solvent by volume). Crystals were grown as previously described (Diller et al., 1994) and a single crystal of dimensions 0.2 × 0.6 × 0.9 mm was used for data collection. The crystal was mounted in a 1.0-mm thin-walled glass capillary using the reservoir solution of the sitting drop vapor diffusion well as a stabilizing solution. Data were collected using CuKα radiation from an Elliot GX-21 rotating anode x-ray generator equipped with focussing mirrors and Mar Research 18-cm-diam image plate scanner. Data were recorded at 18°C. The detector was set at 14 cm from the crystal and 1° oscillations were used with 10-min exposures per frame. A total of 91 frames were collected in 18 h without appreciable crystal decay. The data were indexed, integrated, merged, and scaled with MARXDS (Kabsch, 1988). For 24,754 observations of 7,682 unique reflections the average $I/\sigma(I)$ was 44.4 and Rsymm (I) 5.4%. For the shell 2.8-2.6 Å, the average I/σ (I) was 11.3 and Rsymm (I) 15.2%. The data are 78.9% complete to 2.6 Å and 93.6% complete to 2.8-Å resolution.

The structure was solved by molecular replacement using the Xplor suite of programs (Brünger et al., 1989). The 1.9-Å resolution refined structure of monomeric red abalone sperm lysin was used as a search model (Shaw et al., 1993). The rotation function and Patterson correlation refinement gave two clear solutions, corresponding to each monomer in the dimer. The translation functions for each solution gave 14σ (monomer A) and 10σ (monomer B) peaks. As the two translation solutions were of different peak heights, PC refinement was performed using the dimer model with each monomer being refined as a rigid body. The subsequent translation function for the dimer gave a 21σ peak. Analysis of the packing of the molecular replacement solution showed no bad contacts of the monomers and no bad contacts of symmetry-related molecules. The molecular replacement parameters were optimized by rigid body refinement using data between 10.0–6.0 and 8.0–3.0 Å resolution, resulting in an R-factor of 0.425 for all data with $|F|>3.0\sigma_F$.

The molecular replacement model was refined by positional and simulated annealing using Xplor (Brünger et al., 1989). Positional refinement reduced the R-factor to 25.0% and restrained isotropic individual B-factor refinement further reduced the R-factor to 0.235 for data in the range 8.0–3.0 Å resolution. It was apparent at this stage that the B-factors of monomer B were uniformly higher than for monomer A. To avoid the possibility that close contacts at the dimer interface were preventing correct refinement, residues Arg^{56}, Tyr^{100}, Phe^{101}, Phe^{104}, Asp^{108}, Asn^{109}, Met^{110}, Lys^{113}, and Tyr^{117} were truncated to alanine. Simulated annealing refinement was performed at 1,000°K using 8.0–2.75 Å resolution data with noncrystallographic symmetry restraints applied to the helices of each monomer. A 2|Fo|-|Fc| difference Fourier map based on this model, unbiased at the 18 truncated side chains (nine in each monomer), revealed clear density for 16 of the side chains. The truncated side chains were rebuilt using the program suite Xtalview (McRee, 1993). The 2|Fo|-|Fc| map was used to adjust the model for other residues in each monomer wherever necessary, as the conformation of some of the loops and surface side chains differed in molecule A versus molecule B, and/or differed with respect to the starting model. The model was then refined by simulated annealing as above, followed by restrained B-factor refinement. A subsequent 2|Fo|-|Fc| map revealed density for the two remaining truncated side chains. However, no density was apparent for residues 1-9, 135 and 136 at the NH_2 and COOH termini of each monomer. In addition, Met^{134} is modeled as alanine in each monomer. This map was also used to check and adjust the fit of residues having high B-factors before final simulated annealing and B-factor refinement.

The molecular replacement solution was independently confirmed with a heavy atom derivative. A crystal of dimeric lysin was soaked 18 h in 0.1 mM $KAuCl_4$ in a synthetic mother liquor consisting of the reservoir solution used for crystallization. A complete data set to 2.85 Å resolution was collected and processed as for the native data. The average isomorphous difference was 28% on |F|. The difference Patterson map calculated with data to 4.0 Å resolution contained Harker vectors at $u = 0$, $v = 0$, and $w = 0.5$ (4σ, 4σ, 6σ) consistent with a single site and confirming the space group as $P222_1$. Refinement of the site with Xheavy (McRee, 1993) at 3.0-Å resolution yielded Rcentric of 0.66 and an average phasing power of 1.63. The refined coordinates of the site (0.0129, 0.3915, 0.8821) are consistent with an isomorphous difference Fourier map calculated using phases from the refined model that contains a 14σ peak at ~0.00, 0.40, 0.88, and no other peaks greater than 3σ in the asymmetric unit. The $AuCl_4^-$ anion binds on the local twofold axis between monomers of the asymmetric unit in a hydrophobic pocket formed by the side chains of residues Phe^{52}, Phe^{101}, Leu^{105}, Met^{110}, Pro^{112}, and Met^{118} of each monomer. Charge neutralization is provided by the side chain of Arg^{56} of monomer

B that has contact distances of 4.5 and 5.0 Å to the Au site. The only other contacts to the Au site less than 5.0 Å are from Pro^{112} of each monomer and the carbonyl of Met^{110} of monomer A. Therefore, the Au site is consistent with the difference Patterson map and a difference Fourier map using model based phases. Furthermore, the site is chemically reasonable with respect to the protein structure.

The final model has a R-factor of 0.233 for all 7328 reflections in resolution range 8.0–2.75 Å with $|F| > 0\sigma_F$. The model is comprised of residues 10–134 of each monomer (2,096 atoms total). No solvent molecules have been modeled. The rms deviations from ideality of bonds, angles and planes are 0.023 Å, 4.05°, and 1.73°. As noted below, the average B-factor for molecule A is reduced due to crystal packing contacts. Except for three glycines, there are no outliers in the ϕ,ψ plot. Coordinates have been deposited with the Protein Data Bank (Accession Code 1LYN).

Labeling Lysin with Fluorescent Probes and Fluorescence Energy Transfer Experiments

TRITC and FITC were from Molecular Probes (Eugene, OR). 1 mg of TRITC was dissolved in 200 μl dimethylsulfoxide (11.25 mM stock). A 950-μl aliquot of lysin in natural seawater (pH 7.8) at 3.86 mg/ml was placed in a 1.5-ml microfuge tube and 50 μl of stock TRITC added while vortexing (final TRITC concentration = 0.56 mM). 1 mg FITC was dissolved in 257 μl dimethylsulfoxide (10 mM stock). A 900-μl aliquot of lysin in seawater at 3.86 mg/ml was mixed with 100 μl of FITC stock. Both tubes were incubated 3 h at 23°C and then 50 μl of 2 M glycine added. After 30 min the labeled proteins were separated from the free fluorophores on a 1 × 30-cm column of BioGel-P6 (Bio Rad Laboratories, Richmond, CA) in seawater. The peak void volume fractions were collected and protein determined by the BCA (Pierce) or Lowry assay. The TRITC bound to lysin was quantified using the molar extinction coefficient at 555 nm of 72,000 and for FITC the molar extinction coefficient at 510 nm of 65,000 (Adams et al., 1991). The labeling stoichiometry was 1.1 mol of TRITC and 0.8 mol FITC per mole lysin monomer. The labeled lysins were kept at 4°C in seawater containing 0.04% sodium azide; they retained their ability to dissolve isolated egg VE (Vacquier and Lee, 1993) with the same potency as the unlabeled controls. Lysin is stable indefinitely when stored in seawater/azide at 4°C. The two labeled lysins were combined at least 7 d before experiments, at equal protein concentrations, in various molar ratios of FITC-lysin to TRITC-lysin. For most experiments a molar ratio of 1 FITC: 4 TRITC (one part FITC-lysin plus four parts RITC-lysin, both at equal molar concentrations in seawater [1F+4R]) was selected to maximize the probability that FITC-lysin monomers would dimerize with TRITC-lysin monomers. Fluorescence measurements were done at 23°C in an ISS K2 spectrofluorometer in the photon counting mode using a 5-mm path cuvette to minimize inner filter effects due to the absorption of light by the probes.

Results

Lysin Is a Dimer with Readily Exchangeable Subunits

Cross-linking ^{125}I-lysin with DSP was maximal above 4 μM lysin. Data at 2 μM (33 μg/ml) lysin are shown in Fig 1. The proportion of dimer decreased exponentially below 2 μM lysin. Concentrations of Triton X-100 above 0.03% (0.29 mM; the approximate critical micelle concentration of the detergent) dissociated the dimer (Fig. 1). All detergents tested at concentrations above their critical micelle concentration produced the same results. A control of boiling lysin (at 2 μM monomer) in 1% sodium dodecyl sulfate-seawater, before addition of the cross-linker, showed that ~7% of the radioactivity in the dimer band could be due to the random cross-linking of free monomers. Lysin cross-linked with DSP was inactive at dissolving isolated egg VE.

Subunit interactions between lysin monomers were studied using lysin labeled with fluorescent probes. Direct evidence of dimer formation was obtained from resonance energy transfer from FITC-lysin to TRITC-lysin caused by

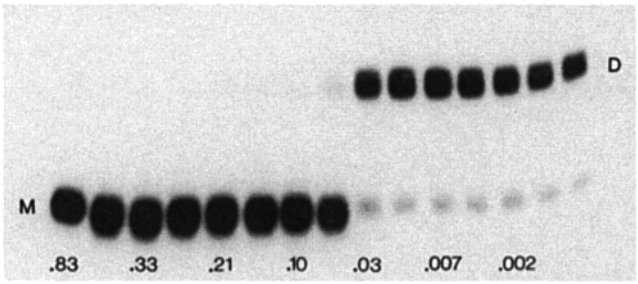

Figure 1. Lysin is a dimer in solution. ^{125}I-Lysin, at 2 μM monomer in seawater, was exposed to the indicated concentrations of Triton X-100 (vol/vol) for at least 30 min and cross-linker added. After 10 min the reaction was stopped with electrophoresis sample buffer. The samples were subjected to SDS-PAGE and autoradiography of dried gels. Triton X-100 dissociates dimers above 0.03%. Similar results were obtained with a variety of detergents. *M* = monomer; *D* = dimer. Approximately 0.5 μg lysin protein was loaded per lane (125,000 cpm).

the close proximity of these two probes within dimers compared to free monomers. Resonance energy transfer was monitored by the decrease in the intensity of the fluorescein peak at 514 nm and the relative increase in the intensity of the rhodamine peak at 573 nm upon dimer formation. The dependence of energy transfer on lysin concentration is shown in Fig. 2 with the spectra normalized to the FITC peak at 514 nm. The energy transfer efficiency decreased, as seen by the decrease in relative intensity at 573 nm, when labeled lysin (1F+4R) was diluted serially with seawater from 16 to 0.125 μM, indicating dissociation of the dimers. Below 250 nM the shape of the spectra

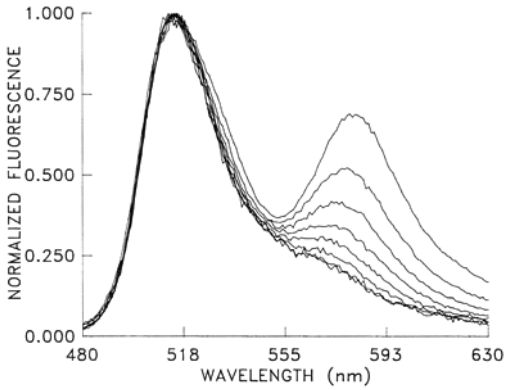

Figure 2. Effect of lysin concentration on energy transfer between monomers. FITC-lysin and TRITC-lysin (both at 16 μM) were mixed together at a molar ratio of 1 FITC-lysin: 4 TRITC-lysin and diluted with seawater at least 7 d before the experiment. Emission spectra of serial 1:1 dilutions with seawater from 16 to 0.125 μM were recorded (excitation 460 nm). The spectra were normalized to the FITC peak emission. Inner filter effects due to the absorbance of the fluorophores contributed to the increase in the 573 nm peaks at 8 and 16 μM monomer. At or below 4 μM, inner filter effects were negligible. The shape of the spectra below 0.25 μM changed little with concentration, suggesting that nearly complete dissociation had occurred. The spectra from highest to lowest intensity at 573 nm correspond to 16, 8, 4, 2, 1, 0.5, 0.25, and 0.125 μM lysin monomer.

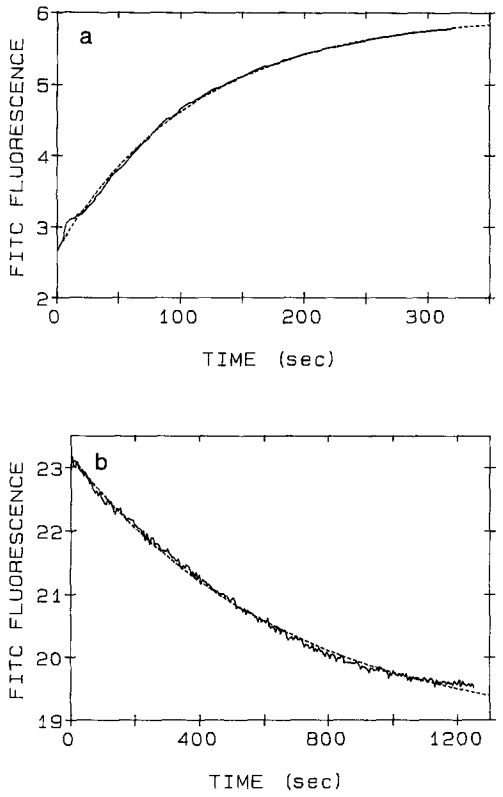

Figure 3. Kinetics of lysin subunit dissociation and exchange. (*a*), Kinetics of lysin dissociation by dilution. 10 μl of 16 μM lysin (1 FITC-lysin + 4 TRITC-lysin; 1F+4R) was added to 490 μl seawater (final concentration 0.32 μM). The time course of the FITC fluorescence change was monitored at 460 nm excitation and 515 nm emission. The solid trace is the experimental data and the dashed line is the fit to a single exponential with rate constant $k = 0.53 \pm 0.01$ min^{-1} ($t_{1/2} = 78$ s). (*b*), Kinetics of lysin subunit exchange. Equal volumes (250 μl) of 8 μM FITC-lysin + unlabeled lysin (1F+4U) and 8 μM TRITC-lysin + unlabeled lysin (4R+1U) were mixed and the time course of the FITC fluorescence change was monitored at 460 nm excitation and 520 nm emission. The solid trace is the experimental data and the dashed line is the fit to a single exponential with rate constant $k = 0.088$ min^{-1} ($t_{1/2} = 7.9$ min).

changed little, suggesting that dissociation was nearly complete. From these data an approximate K_D for dimer formation was calculated to be ~1 μM.

Diluting 16 μM labeled lysin (1F+4R) 50-fold in seawater caused a rapid increase in FITC emission intensity at 520 nm, indicative of dimer dissociation (Fig. 3 *a*). The time course followed a single exponential with a half-time of 78 s. The kinetics of subunit exchange was measured by mixing equal volumes of 8 μM solutions of lysins containing FITC-lysin plus unlabeled (U) lysin (1F+4U), with TRITC-lysin plus unlabeled lysin (1U+4R), and after the decrease in FITC fluorescence at 520 nm indicative of formation of FITC/TRITC lysin dimers (Fig. 3 *b*). The time course followed a single exponential with a half time of 7.9 min. Comparison of the emission spectra at equilibrium showed that inclusion of unlabeled lysin decreased the efficiency of energy transfer between FITC-lysin and TRITC-lysin, indicating that unlabeled lysin competes with labeled lysin for dimer formation. The above results demonstrate that lysin dimers dissociate and exchange monomers rapidly.

Crystal Structure of the Dimer

The molecular structure of lysin crystals grown at pH 7.0, refined at 1.9 Å resolution, revealed lysin monomers packed with one molecule per asymmetric unit (Shaw et al., 1993). Association of lysin monomers at neutral pH involves extensive crystal packing contacts between the hydrophobic residues of the extended NH_2-terminal domain of one monomer, with a cluster of solvent-exposed hydrophobic residues of an adjacent lysin molecule. However, in the crystals grown at pH 5.5 described herein, the lysin monomers self-associate via the surface cluster of hydrophobic residues to form a lattice with one dimer per asymmetric unit. Previous measurements of dynamic light scattering of solutions of purified lysin at 14 mg/ml (870 μM) at pH 4.5 and 5.5 showed essentially all the lysin to be dimeric with an estimated molecular weight of 38.2 kD (Diller et al., 1994). This result is consistent with the data in Figs. 1 and 2, showing that lysin forms dimers.

The dimer exhibits an extended S shape when viewed along the direction of the local 2-fold axis relating the monomeric helical bundles (Fig 4 *a*). The overall dimensions of the dimer are ~80 × 40 × 30 Å. There is a cleft ~20 Å wide and 15 Å deep on opposite sides of the twofold axis. When viewed from the side (perpendicular to the local twofold axis) the dimer is essentially flat on one surface, while the opposite surface is convex (Fig. 4 *b*). When viewed end-on the dimer displays a marked asymmetric clustering of the residues of the hydrophobic patches (Fig. 4 *c*).

The packing of lysin in the pH 5.5 crystal form is lamellar with dimers forming infinite sheets in the **bc** plane of the unit cell. The twofold axis relating monomers is approximately normal to this sheet, and the sheets are separated by solvent channels. There are relatively few contacts across the solvent channels. Consequently, the many

Figure 4. Three orthogonal views of the crystal structure of dimeric *H. rufescens* sperm lysin. α-Helices are red and NH_2- and COOH-terminal domains are blue. The side chains of 22 Arg and Lys residues of each monomer are shown (C atoms *dark blue*; N atoms *lavender*). Arg^1, Lys^9, and Lys^{136} of each monomer are not visible in the crystal structure. The side chains of 11 residues of each monomer that comprise the interacting hydrophobic patches are shown (atoms are colored: C, *green*; O, *red*; N, *lavender*; S, *yellow*). These 11 residues are Tyr^{57}, Tyr^{65}, Leu^{67}, Trp^{68}, Ile^{92}, Ile^{96}, Met^{98}, Tyr^{100}, Phe^{101}, Phe^{104}, and Met^{110} (Shaw et al., 1993). (*a*) The view along the local 2-fold axis relating monomers of the dimer. In this view molecule A is to the lower left and molecule B is to the upper right. On molecule A the NH_2 terminus at residue 10 is below the COOH terminus at residue 134 (adjacent to Lys^{132}). (*b*) The view perpendicular to the local twofold axis, i.e., from the right side of the view in (*a*), showing that one surface of the dimer is essentially flat, while the opposite surface is convex. (*c*) End on view of the dimer, i.e., from the bottom of the view in (*a*), showing that residues of the hydrophobic patches, which participate extensively in the dimer interface, are clustered on one side of the dimer. This feature of the structure is also seen in (*b*). The figures were made with the program Molscript.

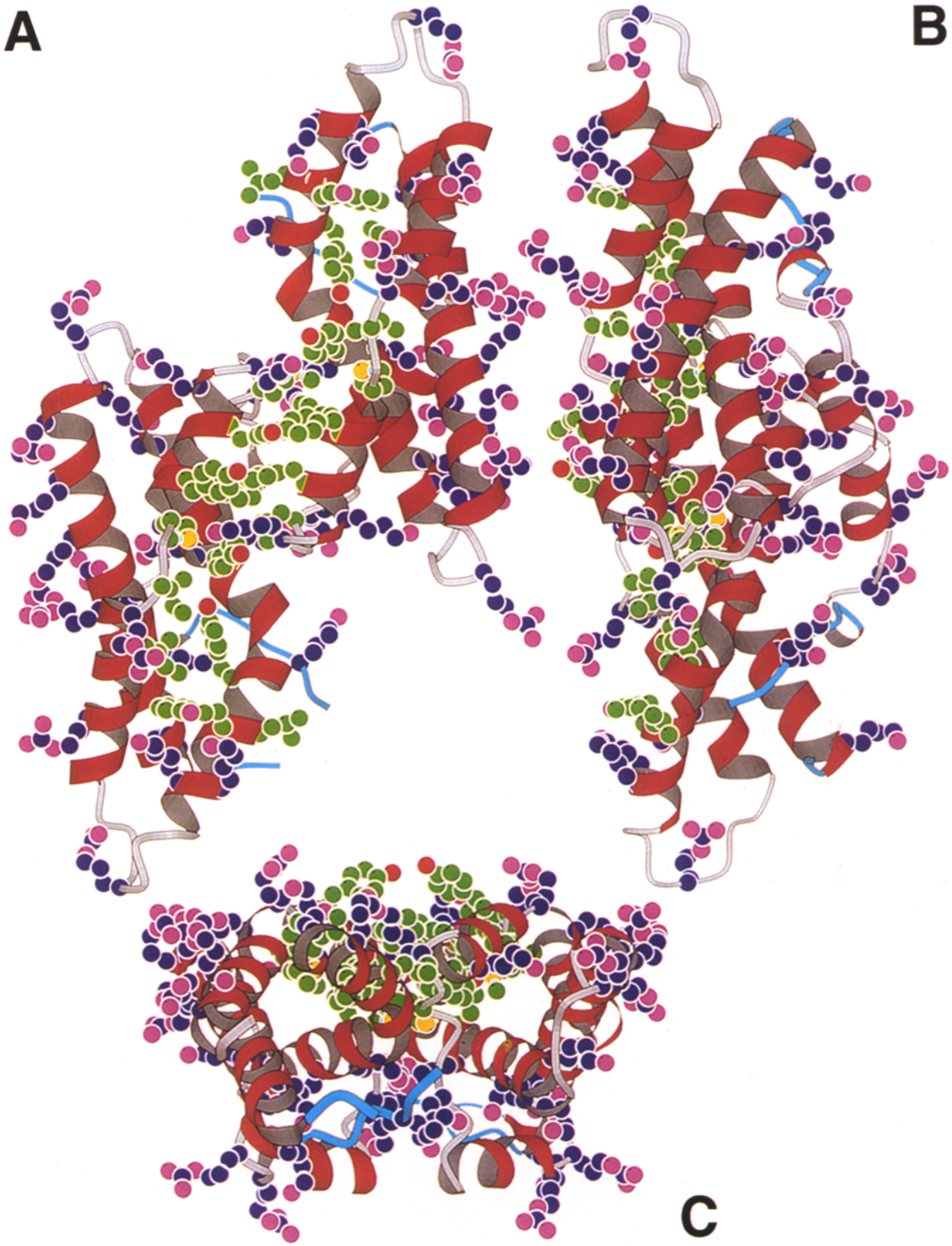
A
B
C

positively charged residues on the surface of the dimer are shielded from each other in the crystal. There are two packing contacts involving acidic residues. One involves the side chains of Asp^{128} on symmetry-related molecules, and the other involves Glu^{16} and Glu^{120} on symmetry-related molecules. Presumably, these contacts are able to occur at pH 5.5, but not at pH 7.0, explaining why dimers are not observed in crystals grown at pH 7.0.

The individual molecules of the lysin dimer (A and B) have different crystal packing environments. Molecule A has nine contacts (salt bridges or hydrogen bonds) involving 10 residues to symmetry-related A or B molecules via two of the crystallographic twofold axes, whereas molecule B has six such contacts involving five residues and only one crystallographic twofold axis. Consequently, molecule B, having relatively few contacts compared to A, is incorporated into the lattice primarily by virtue of interaction with molecule A. Consistent with the crystal packing environment, the average temperature factor for molecule B is higher than for molecule A, 20.3 $Å^2$ versus 13.2 $Å^2$. By comparison, the average temperature factor for monomeric lysin (M) in crystals grown at pH 7.0 is 20.9 $Å^2$ (Shaw et al., 1993), suggesting that the average temperature factor of molecule A is reduced due to constraints of the crystal lattice.

Comparison of the structures of A, B, and M molecules shows that lysin has a relatively rigid helical bundle structure with flexible loops and connecting chain segments, and highly flexible NH_2 and COOH termini.

Least squares fit of all Cα atoms results in the following rms differences: A vs. M, 0.69 Å; A vs. B, 0.61 Å; B vs. M, 0.57 Å. However, least squares fit of 88 Cα atoms in the five α-helices yields rms deviations in the range of 0.39-0.49 Å for these three comparisons, showing that the helical bundle is very similar in all three molecules. Residues that differ at Cα by more than two-times the rms difference predominantly reside in the interhelical segments and loops, including residues 10, 11, 38–40, 74, 75, 78, 79, 96–100, 107–110, and 132–134. The side chain conformations of some of these residues also differ significantly, in particular for Phe^{10}, His^{38}, Arg^{40}, Ile^{96}, Asp^{97}, Tyr^{100}, Phe^{104}, Lys^{108}, Met^{110}, and Tyr^{133}. In addition, the NH_2-terminal residues 1–9 are completely disordered in the lysin dimer, while residues 4–9 remain ordered in the monomer. The COOH-terminal residues Gly^{135} and Lys^{136} are disordered in the structures of A, B, and M molecules. Temperature factors are also consistently higher for the interhelical and terminal regions compared to helical segments.

Lysin dimerizes via its exposed hydrophobic patch. Altogether, 12 residues of each monomer are involved in contacts of less than 3.5 Å at the dimer interface (Fig. 5 *a*). The interactions primarily involve hydrophobic and aromatic side chains. The central feature of the interface is a stack of aromatic residues in which Phe^{101} and Phe^{104} of molecule A and B intercalate with each other. Listing them in order, the stack is comprised of His^{61}, Tyr^{57}, Phe^{101}, $Phe^{104'}$, Phe^{104}, $Phe^{101'}$, $Tyr^{57'}$, and $His^{61'}$ (prime indicates residues on molecule B; see Fig. 5 *b*). The intercalation of $Phe^{104'}$ between Phe^{101} and Phe^{104} resembles the stacking of Phe^{10} on Phe^{104} between monomers (Shaw et al., 1993). Flanking this stack are Met^{110}, $Met^{110'}$, Tyr^{100}, $Tyr^{100'}$, Lys^{108}, and $Lys^{108'}$. The Tyr and Lys side chains shield the central four Phe residues of the stack from solvent. Additional hydrophobic contacts involve the side chains of Lys^{113}, $Tyr^{117'}$, $Lys^{113'}$and Tyr^{117}. There are only two hydrogen bonds in the dimer interface, one between the side chain of Arg^{56} and the carbonyl of $Ile^{111'}$, (2.85 Å) and the other between the side chain of $Lys^{108'}$ and the carbonyl of Asp^{97} (2.68 Å). The reciprocal interactions on the opposite side of the dimer 2-fold axis cannot occur because the contact distances are greater than 5 Å. Polar contacts shorter than 3.5 Å involving His^{61}, Lys^{108}, and Asn^{109} occur, but do not have the proper geometry for hydrogen bonding. Altogether, of 20 contacts at the dimer interface, 14 are hydrophobic or stacking interactions, two are specific hydrogen bonds and four are nonspecific polar interactions. These contacts are not distributed symmetrically: there are 15 for molecule A to molecule B, but only five for molecule B to molecule A on the opposite side of the dimer twofold axis. The asymmetry is accommodated by alternate conformations of the side chains, and by the

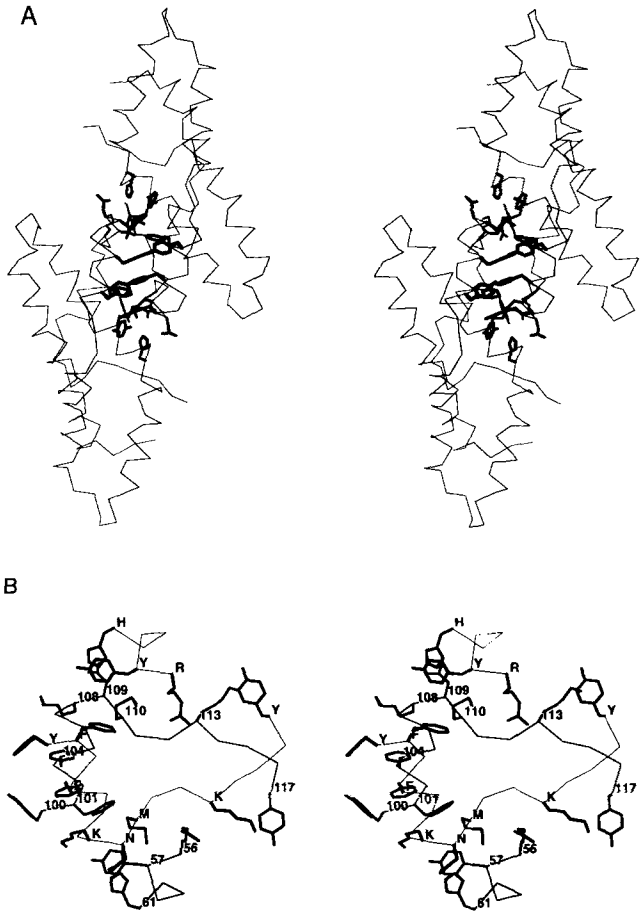

Figure 5. Stereo figures highlighting the side chains of residues of each monomer that are involved in the dimer interface. (*a*) View of the dimer as in Fig. 4 *a*, showing the Cα atoms of each monomer (connected with thin lines) and the side chains of dimer interface contact residues (*thick lines*). (*b*) Closeup of the dimer interface contact residues viewed as in Fig. 4 *b*, i.e., the local twofold axis is horizontal and in the plane of the figure. Residues on molecule A are labeled at their Cα atoms by residue number, while residues on molecule B are labeled at their Cα atoms using the single letter amino acid code.

fact that most of the residues involved reside on, or are adjacent to, the flexible interhelical segments of residues 95–99 and 107–116. The asymmetry may result from the different crystal packing environments of A and B molecules.

A central feature of the dimer interface is the association of five residues, Tyr^{57}, Tyr^{100}, Phe^{101}, Phe^{104}, and Met^{110}, within the hydrophobic patch of each monomer, which shields their side chains from solvent (Fig. 5 *b*). The total surface area buried per monomer due to dimerization is 669 Å^2 as computed with a 1.4-Å probe sphere (Connolly, 1983). Of this total area, 276 Å^2, or 41% per monomer, arises from these five residues alone. The remaining residues of the hydrophobic patch contribute only 5 Å^2 per monomer to the total buried surface area. Consequently, in the lysin dimer a significant portion of the hydrophobic patch remains exposed (~310 Å^2 per monomer). Thus only about half of the hydrophobic patch is involved in forming the dimer. Other residues involved in the interface, in addition to the above mentioned five, contribute another 191 Å^2, or 29%, of the total buried surface area. The remaining 30% (202 Å^2) represents cavities within the dimer interface that are inaccessible to the 1.4-Å probe sphere.

The lysin dimer interface is fairly typical of other protein–protein interactions both in terms of total surface area and the proportion of polar and nonpolar residues involved, although there are only two hydrogen bonds in the lysin dimer (Janin and Chothia, 1990; Chacko et al., 1995). An unusual feature of the lysin dimer interface is the intercalation of Phe^{101}, $Phe^{104'}$, Phe^{104}, and $Phe^{101'}$, which provides specificity to the interaction of monomers due to shape complementarity. A dimer interface with this characteristic, i.e., complementary surfaces of hydrophobic residues, is observed in the dissociable dimer of *Chromatium vinosum* cytochrome c (Ren et al., 1993). The specific interaction of the Phe residues in the lysin dimer also resembles the interaction of human growth hormone with its receptor. In this case two Trp residues of the receptor and to a lesser extent three Ile and a Pro at the center of the interface, are involved in contacts that provide the majority of the binding energy stabilizing the complex (Clackson and Wells, 1995). By analogy, one could expect that the majority of binding energy in the lysin dimer arises from intercalation of the Phe^{101} and Phe^{104} residues, in combination with the association of Tyr^{57}, Tyr^{100}, and Met^{110} residues of each monomer.

Red abalone sperm lysin is a remarkably basic protein with 12 Arg and 13 Lys residues out of 136 amino acids (Vacquier et al., 1990). In the structure of the monomeric protein, 23 of these residues are arranged in two separate, approximately parallel, tracks running the length of the molecule (Shaw et al., 1993). In the structure of the dimer, 22 of these basic residues are ordered in each monomer, resulting in an array of 44 Arg and Lys side chains on the surface of the dimer (Fig. 6). The basic tracks lie on opposite sides of the dimer. Furthermore, they are approximately equidistant from the dimer interface. The arrangement of the basic tracks in the dimer is apparent in Fig. 4 *c*. As viewed in Fig. 6, the tracks comprised of residues 29, 33, 36, 71, 72, 78, 87, 94, and 95 lie toward the front of each monomer, and those comprised of residues 13, 20, 40, 47, 48, 55, 106, 123, and 125 lie toward the back. Four residues

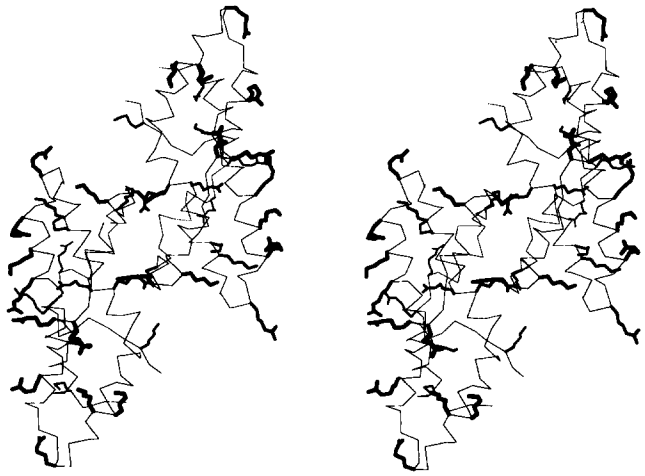

Figure 6. Stereo figure highlighting 22 basic residues of each monomer (11 Arg and 11 Lys) in the lysin dimer. The view of the dimer is the same as in Figs. 4 *a* and 5 *a*. The Cα atoms of each monomer are connected with thin lines; the Arg and Lys side chains are shown with thick lines. Arg^1, Lys^9, and Lys^{136} of each monomer are not visible in the crystal structure.

associated with this latter group, Arg^{56}, Lys^{108}, Lys^{113}, and Lys^{132} are offset from the essentially linear array of the rest of the side chains in this track; they lie closer to the dimer interface. In fact, the first three of these residues participate in dimer interface contacts. Arg^1 and Lys^{136} (the two termini of each monomer) and Lys^9 are not visible in the crystal structure of the dimer. These residues could be expected to be juxtaposed to the basic tracks at the back of the dimer as viewed in Fig. 6. Including these residues, the lysin dimer has a net charge at pH 7 of +26.

Vitelline Envelopes Dissociate Lysin Dimers

The addition of VE to lysin dimers labeled with both probes (1F+4R) resulted in a concentration dependent loss of energy transfer as seen 10 min after VE addition by the decrease in the relative intensity of the TRITC peak at 573 nm (Fig. 7). The time course of the VE-induced loss of energy transfer was monitored as the increase in FITC emission at 520 nm; it followed a single exponential with a rate constant of 1.4 min^{-1} (Fig. 8). These data show that the VEs dissociate lysin dimers and suggest that the monomer is the active species in the dissolution reaction. Furthermore, fluorescence polarization measurements indicated that the rotational motion of monomers labeled with either fluorophore decreased upon addition of VEs, suggesting that the monomer was bound tightly to VE protein (data not shown). These data are in accord with the original observation that lysin binding to the VE molecules is an irreversible process (Lewis et al., 1982).

Discussion

When the structure of monomeric red abalone sperm lysin was resolved it revealed three striking features associated with its surface: two tracks of basic residues, a large, exposed hydrophobic patch, and the clustering of residues that are hypervariable among species (Shaw et al., 1993, 1994). This paper presents the crystal structure of the ho-

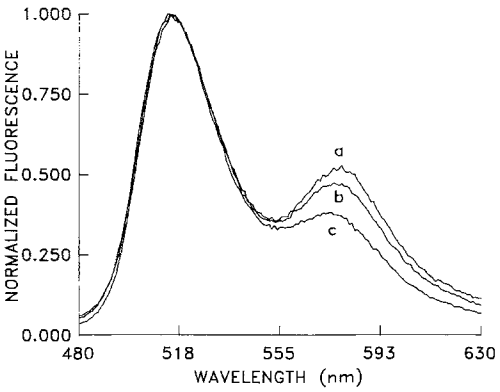

Figure 7. Effect of VEs on energy transfer between monomers. Spectra are normalized to the FITC peak emission. Lysin (500 μl) was at 8 μM (1 FITC-lysin + 4 RITC-lysin). Energy transfer was measured before (*a*) and 10 min after (*b* and *c*) the addition of 50 μl (*b*) and 100 μl (*c*) of a seawater suspension of isolated egg VEs (~11 μg of VE protein per 50 μl VE suspension). The decrease in the peak emission at 580 nm indicates decreased energy transfer, i.e., dimer dissociation (excitation 460 nm; 23°C).

modimeric form of lysin. In the dimer the hydrophobic patch is ~50% occluded, while the number of basic and hypervariable (among species, Lee et al., 1995) residues on the surface is doubled. It is unclear at this time as to what factors affect the crystallization of lysin into either the monomer or the dimer form; however, pH may be an important factor. Nevertheless, the two crystal structures provide independent, consistent images of this fertilization protein.

Our objective is to understand the nonenzymatic mechanism by which lysin dissolves the egg VE. This is a key event in abalone fertilization. Because the abalone egg VE is a fibrous glycoproteinaceous structure, as is the mammalian egg zona pellucida, the study of abalone sperm lysin may provide relevant clues to the mechanism of penetration of the mammalian zona by mammalian sperm.

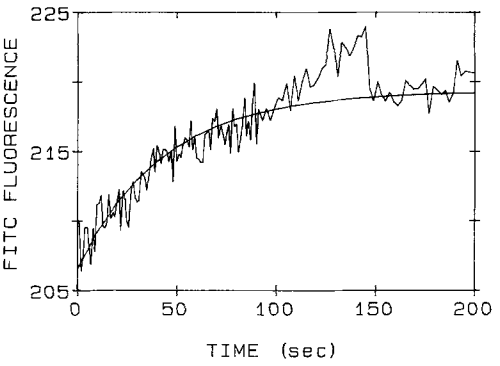

Figure 8. Kinetics of lysin dimer dissociation by egg VEs. 500 μl of 8 μM lysin (1 FITC-lysin + 4 TRITC-lysin) was placed in a cuvette and 100 μl VE suspension added (~22 μg protein. The time course in the fluorescence intensity increase at 520 nm was monitored (excitation at 460 nm). The jagged trace are the actual data, and the smooth trace the fit of the data to a single exponential with a rate constant, $k = 1.4 \pm 0.1\ \text{min}^{-1}$ ($t_{1/2} = 30$ s). The fluctuations in intensity are artifacts caused by the VEs passing through the light path.

This paper provides new information about the function of lysin by showing that it is a dimer in solution that monomerizes during, or immediately after, its contact with the VE. Lysin is a major protein of abalone sperm cells that is released in a highly concentrated form onto the VE (Lewis et al., 1982). The exact concentration of lysin on the VE at the point of sperm contact is unknown, but certainly it is greater than 62 μM (1 mg/ml). Measurements of dynamic light scattering of lysin at 14 mg/ml (870 μM) showed lysin to be a dimer (Diller et al., 1994). At much lower lysin concentrations, the cross-linking and fluorescence energy transfer data also show that lysin is a dimer. The data indicate that monomers exchange rapidly between dimers (Fig. 3), and at concentrations below ~0.25 μM, dimer dissociation is nearly complete (Fig. 2). Most importantly, the fluorescence energy transfer data show that dimers dissociate in the presence of the VE (Figs. 7 and 8).

Because lysin binds the VE as a monomer, or monomerizes after binding, the previous analysis of the surface features of the protein must be considered. The function of the basic tracks may be to cleave hydrogen bonds between glycoprotein molecules (Lewis et al., 1982) comprising the VE, whereas the function of the hydrophobic patch may be to disrupt hydrophobic interactions (Shaw et al., 1993, 1994). Until more is known about the interaction of the VE and lysin, each hypothesis, or their combination, should be considered as plausible. The available data strongly implicate the NH_2-terminal domain of residues 1–12 as being responsible for species-selective recognition (Shaw et al., 1993, 1994; Lee et al., 1995). At this time, the remarkable sequence conservation among 20 species of the residues comprising both the basic tracks and the hydrophobic patch (Lee et al., 1995) supports the idea that both these surface features are involved in the dissolution mechanism. Thus, we envision a minimum of three separate interactions between lysin and the VE. The first is mediated by the two NH_2 termini of the dimer and are species selective. This species recognition allows for the "proper fit" of the dimer with certain VE molecules; this results in the second step that is the dissociation of the dimer. The third step is mediated by either or both the hydrophobic patch and the basic tracks, the result being that the 13-nm-diam fibers comprising the VE loose cohesion and unravel (Lewis et al., 1982; Mozingo et al., 1995). While the first step shows species-selectivity, steps two and three are general to all abalone sperm lysins. DSP cross-linked lysin is inactive at dissolving egg VE. Although consistent with the idea that the monomer is the active species, DSP would also react with the amino groups of the 13 Lys residues of each monomer and may thus destroy the function of the basic tracks. Although the work in this paper has utilized lysin from the red abalone (*H. rufescens*), lysin from two other California species (*H. cracheroidii* and *H. corrugata*) also exist in solution as dimers and yield the same cross-linking pattern as that shown in Fig. 1.

The presence of the hydrophobic patch on the opposite surface of the monomer from the basic tracks imparts to lysin a net hydrophobic dipole, or amphipathic character. The amphipathic character of lysin imparts on the protein the ability to be a potent fusagen of artificial lipid vesicles (Hong and Vacquier, 1986). While this property may be important in the dissolution of the VE, it also promotes

self association of monomers. The structural data argue that this is a stereo specific, rather than random, interaction. The hydrophobic surfaces of the dimer interface have complementary shapes and in particular there is a striking intercalation involving four Phe residues. Thus, an important function for the hydrophobic patch, not apparent from the structure of the monomer alone, is to mediate stereo-specific interaction of monomers.

If the monomer is the active form of lysin, what could be the importance of the existence of the dimeric lysin before its interaction with the VE? One possibility is that in the dimer form, the amphipathic character of lysin is neutralized, providing a water soluble protein that can be delivered in high concentration in a high ionic strength aqueous medium (seawater). An alternative possibility is that dimerization is important in the packaging of lysin in the acrosomal granule (Lewis et al., 1980; Haino-Fukushima and Usui, 1986). The crystal packing structure of the lysin dimer shows that the basic tracks on adjacent dimers are shielded from each other by extensive solvent channels. A similar arrangement in the acrosome would optimize the packing of the very basic molecules at physiological ionic strength.

A third potential reason for the existence of the dimer is implied by its dissociation in the presence of the VE. The dimer could shield the hydrophobic patch from nonspecific interaction with other hydrophobic domains of cellular components. Upon exocytosis of the lysin directly onto the VE (Lewis et al., 1982), the low affinity association of monomers, and molecular recognition of lysin with the VE, results in dimer dissociation and exposure of the hydrophobic patch inside the fibrous matrix of the VE (Mozingo et al., 1995). Dimerization thus may protect the hydrophobic patch until contact between the dimer and the VE is made. Support for this idea comes from the fact that ^{125}I-lysin binds tenaciously to paraffin coated microfuge tubes. Unlabeled lysin competes with labeled protein in binding to paraffin. Once bound to paraffin, 5% vol/vol Triton X-100 will not displace lysin. However, the presence of low concentrations of Triton X-100 (0.02%) will prevent lysin from binding to paraffin. Once bound to paraffin, 5% SDS will displace the protein from the paraffinized tube (Vacquier, V. D., unpublished data). The hydrophobic patch is the only domain of the lysin molecule that could bind to paraffin since the remainder of the surface of lysin is highly polar. These data indicate that the hydrophobic patch can bind tightly, and nonspecifically, to other hydrophobic molecules. This property may explain why lysin binds irreversibly to VE molecules.

Because Triton X-100 will dissociate dimers we determined the effect of this detergent on the ability of lysin to dissolve VE; concentrations above 0.03% were partially inhibitory. For example, at detergent concentrations between 0–0.02%, 63 μg of lysin were required to dissolve 50% of the isolated VEs, whereas at 0.04%, 105 μg lysin was required. Although showing that the monomer is active in the presence of Triton X-100, such experiments do not distinguish if the inhibitory effect of the detergent involves its binding to the VE, to lysin, or to both. Future experiments will be directed toward identifying the components of the VE to which lysin binds and at understanding the chemical nature of their interaction.

We thank J. D. Bleil for helpful discussions and M. Pique for solvent accessibility calculations.

This work was supported by National Science Foundation grant MCB-9205020 to C. D. Stout, National Institutes of Health grant GM-47165 to P. A. G. Fortes and HD-12986 to V. D. Vacquier.

Received for publication 31 March 1995.

References

Adams, S. R., A. T. Harootunian, Y. J. Buechler, S. S. Taylor, and R. Y. Tsien. 1991. Fluorescence ratio imaging of cyclic AMP in single cells. *Nature (Lond.).* 349:694–698.

Brünger, A. T., J. Kuriyan, and M. Karplus. 1989. Crystallographic R factor refinement by molecular dynamics. *Science (Wash. DC).* 235:458–463.

Chacko, S., E. Silverton, L. Kam-Morgan, S. Smith-Gill, G. Cohen, and D. Davies. 1995. Structure of an antibody-lysozyme complex: unexpected effect of a conservative mutation. *J. Mol. Biol.* 245:261–274.

Clackson, T., and J. A. Wells. 1995. A hot spot of binding energy in a hormone-receptor interface. *Science (Wash. DC).* 267:383–386.

Connolly, M. L. 1983. Solvent-accessible surfaces of proteins and nucleic acids. *Science (Wash. DC).* 221:709–713.

Diller, T. C., A. Shaw, E. A. Stura, V. D. Vacquier, and C. D. Stout. 1994. Acid pH crystallization of the basic protein lysin from the spermatozoa of red abalone (*Haliotis rufescens*). *Acta Crystallogr. D. Biol. Crystallogr.* 50:620-626.

Haino-Fukushima, K., and N. Usui. 1986. Purification and immunocytochemical localization of the vitelline coat lysin of abalone spermatozoa. *Dev. Biol.* 115:27–34.

Hong, K., and V. D. Vacquier. 1986. Fusion of liposomes induced by a cationic protein from the acrosome granule of abalone spermatozoa. *Biochemistry.* 25:543–549.

Janin, J., and C. Chothia. 1990. The structure of protein-protein recognition sites. *J. Biol. Chem.* 265:16027–16030.

Kabsch, W. 1988. Automatic indexing of rotation diffraction patterns. *J. Appl. Crystallogr.* 21:67–71.

Laemmli, U. K. 1970. Cleavage of structural proteins during the assembly of the head of bacteriophage T-4. *Nature (Lond.).* 277:680–685.

Lee, Y.-H. 1994. Abalone sperm lysin: molecular evolution of a fertilization protein, implications concerning the species-specificity of fertilization in marine invertebrates. Ph.D. Thesis, University of California, San Diego. 149 pp.

Lee, Y.-H., T. Ota, and V. D. Vacquier. 1995. Positive selection is a general phenomenon in the evolution of abalone sperm lysin. *Mol. Biol. Evol.* 12: 231–239.

Lewis, C. A., D. L. Leighton, and V. D. Vacquier. 1980. Morphology of abalone spermatozoa before and after the acrosome reaction. *J. Ultrastruct. Res.* 72: 39–46.

Lewis, C. A., C. F. Talbot, and V. D. Vacquier. 1982. A protein from abalone sperm dissolves the egg vitelline layer by a nonenzymatic mechanism. *Dev. Biol.* 92:227–239.

McRee, D. E. 1993. Practical Protein Crystallography. Academic Press, San Diego. 386 pp.

Mozingo, N. M., V. D. Vacquier, and D. E. Chandler. 1995. Structural features of the abalone egg extracellular matrix and its role in gamete interaction during fertilization. *Mol. Reprod. Dev.* In press.

Ren, Z., T. Meyer, and D. E. McRee. 1993. Atomic structure of a cytochrome c' with an unusual ligand-controlled dimer dissociation at 1.8Å resolution. *J. Mol. Biol.* 234:433–445.

Shaw, A., D. E. McRee, V. D. Vacquier, and C. D. Stout. 1993. The crystal structure of lysin, a fertilization protein. *Science (Wash. DC).* 262:1864–1868.

Shaw, A., Y.-H. Lee, C. D. Stout, and V. D. Vacquier. 1994. The species-specificity and structure of abalone sperm lysin. *Semin. Dev. Biol.* 5:209–216.

Vacquier, V. D., K. R. Carner, and C. D. Stout. 1990. Species-specific sequences of abalone lysin, the sperm protein that creates a hole in the egg envelope. *Proc. Natl. Acad. Sci. USA.* 87:5792–5797.

Vacquier, V. D., and Y.-H. Lee. 1993. Abalone sperm lysin: unusual mode of evolution of a gamete recognition protein. *Zygote.* 1:181–196.